Experimentally derived rate coefficients for electron ionization, attachment and detachment as well as ion conversion in pure O2 and N2-O2 mixtures

Experimentally derived rate coefficients for electron ionization, attachment and detachment as well as ion conversion in pure O2 and N2-O2 mixtures

Experimentally derived rate coefficients for electron ionization, attachment and detachment as well as ion conversion in pure O2 and N2-O2 mixtures

P Haefliger, A Hösl and C M Franck

Power Systems and High Voltage Laboratories, ETH Zurich, Physikstr. 3, 8092 Zurich, Switzerland

E-mail: cfranck@ethz.ch

Abstract.

We obtain rate coefficients for mixtures of O_2 and N_2 as well as pure O_2, by fitting pulsed Townsend measurements over a large pressure range from 3 kPa to 100 kPa in a density-reduced electric field range from 40 to 110 Td (1 Td = 10^{-21} Vm^2). The applied model includes ionization, dissociative attachment to O^- and non-dissociative attachment to O_2^-, O^- and O_2^- detachment, as well as charge transfer and ion conversion from O^- to O_2^- and O_3^-. The results are compared to Bolsig+ and MAGBOLTZ simulations and experimental data, where available. The key novelty is the simultaneously obtained rate coefficients from a single Pulsed Townsend experiment including several ion processes over the whole N_2-O_2 mixing range.

PACS numbers: 00.00, 20.00, 42.10

Submitted to: *J. Phys. D: Appl. Phys.*

1. Introduction

Electron swarm parameters in nitrogen-oxygen mixtures are of great interest in atmospheric physics [1], pollution control [2] or for application as electrical insulation media, which is our focus. Most gas insulated switchgear nowadays contain SF_6, which has supreme insulation and arc quenching properties, but is an extremely potent greenhouse gas. Mixtures of N_2, O_2 and CO_2 at high pressures, with an optional admixture of a fluorinated gas, are under investigation for replacing SF_6 [3, 4, 5, 6]. This publication aims at investigating the physical behaviour of N_2 and O_2 mixtures in order to predict and optimize their electric strength. On the subject of oxygen or air, various authors presented experimental [7, 8, 9, 10, 11, 12, 13, 14, 15, 16] and theoretical work [17, 18], which differ with regard to the physical model. In a previous publication [19] we presented a literature review about the physical processes involved,

and used a simplified model of van der Laan and Verhaart [20] with two negative ion species to fit our pulsed Townsend measurements in dry air (79% N_2 and 21% O_2).

For measurements at higher O_2 concentrations, we found that the previously applied model needed to be extended by additional ion processes in order to achieve a satisfying agreement between the measured currents and the simulation results. The extended model distinguishes between O^- and O_2^- ions, and introduces individual electron attachment, detachment and ion conversion rate coefficients. The present model explains all measurements with different gas mixtures and pressures of up to 100 kPa, including measurements of pure oxygen with traces of hydrogen. We report rate coefficients for several processes in N_2-O_2 gas mixtures for the first time. In case of the detachment from O_2^- our results support the results of Neill and Craggs [8], while disagreeing with those of Frommhold [9].

We briefly review the experimental setup and fitting routine in sections 2 and 4. Subsequently, the relevant electron and ion processes of the model are discussed in section 3. In section 5 the results are compared to available literature data, which is mostly measurements in pure O_2.

2. Experimental setup

The gases are measured with a pulsed Townsend experiment, described in detail in [21]. The recently built up experiment was optimized towards electrical field homogeneity and accuracy in distance. The accumulated error from the various experimental parameters is smaller than $\pm 0.5\%$ in the density-reduced electric field E/N. The displacement current of electrons and ions is measured with a high speed current amplifier and connected in cascade with a wide-band voltage amplifier, yielding a total gain of 50 k at a bandwidth from DC up to 200 MHz. The electron source is a photocathode coated with a thin metal film, and back illuminated by a Nd-Yag laser of 266 nm wavelength and 1.5 ns FWHM pulse duration. The efficiency of most films decreases drastically in the presence of oxygen. Having experimented with several materials, a double thin film layer coating of magnesium and palladium showed the most stable efficiency. To avoid the influence of space charge the laser beam is expanded to the full photocathode surface area of 25 mm diameter, while the total charge is controlled and limited to 10 pC. The chamber has a vacuum base pressure of 5 μPa. The utilized gases N_2 and O_2 have a purity of 6.0 and 5.0.

3. Kinetic model

In [19] we have used the model of kinetic processes presented by Verhaart and van der Laan [20] to extract rate coefficients for dry air (N_2-O_2 mixture of 79-21%). We found that this simple model is insufficient for higher O_2 concentrations. Based on a literature study we choose the kinetic model as shown in fig. 1, and find this model suitable for all mixing ratios, including pure O_2 with and without traces of hydro-

gen. The main extension is the explicit simulation of three negative ion species: O^-, O_2^- and O_3^-. Similar models with slight variation have been used by various authors [17, 10, 22, 23, 24, 8, 25, 26, 12] for O_2 and $N_2 - O_2$ mixtures.

The individual processes are as follows:
N_2 and O_2 ionization at 15.5 eV [27] and 12 eV [28] are modeled by a single ionization rate ν_i, equation (1). Since charge transfer from N_2^+ to O_2^+ is known to be efficient for ions at thermal energies [29, 30], only one positive ion species (O_2^+) is modeled.

$$M + e^- \overset{\nu_\mathrm{i}}{\rightarrow} M^+ + 2e^- \tag{1}$$

Discharges in oxygen show both dissociative attachment to O^- (2) and three body attachment to O_2^- (3), where the third collision partner M in (3) is either N_2 (low efficiency [29]) or O_2.

$$O_2 + e^- \overset{\nu_\mathrm{a}^O}{\rightarrow} O^- + O \tag{2}$$

$$O_2 + e^- + M \overset{\nu_\mathrm{a}^{O2}}{\rightarrow} O_2^{-*} + M \rightarrow O_2^- + M \tag{3}$$

O^- ions exhibit detachment by reaction with N_2 (4) and formation of N_2O. In pure oxygen, detachment is equally observed at a comparably lower rate. O^- ions can further be converted to O_2^- (5) or, via a three-body process, to O_3^- (6).

$$O^- + N_2 \overset{\nu_\mathrm{d}^O}{\rightarrow} N_2O^{-*} \rightarrow N_2O + e^- \tag{4}$$

$$O^- + O_2 \overset{\nu_\mathrm{c}^{O2}}{\rightarrow} O_3^{-*} \rightarrow O + O_2^- \tag{5}$$

$$O^- + O_2 + M \overset{\nu_\mathrm{c}^{O3}}{\rightarrow} O_3^{-*} + M \rightarrow O_3^- + M \tag{6}$$

Finally, detachment of O_2^- ions is observed as (7):

$$O_2^- + M \overset{\nu_\mathrm{d}^{O2}}{\rightarrow} O_2 + M + e^- \tag{7}$$

In literature clustering processes both for positive and negative ions are sometimes considered [30, 31, 32, 33]. We omit them due to the lack of sensitivity of our measurements to these processes.

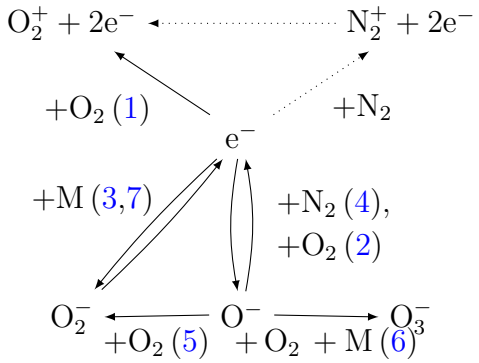

Figure 1: Overview of the relevant processes used for rate determination in this contribution. We neglect interactions with excited molecules. The dotted line processes are part of process (1) as a distinction of different ionization processes based on our measurements is impossible.

This kinetic model transcribes into the following system of partial differential equations where $\rho(x,t)^y$ is the number density of species y and w^y its drift velocity:

$$\frac{\partial}{\partial t}\begin{pmatrix}\rho^{\mathrm{e}}(x,t)\\ \rho^{\mathrm{O_2^+}}(x,t)\\ \rho^{\mathrm{O^-}}(x,t)\\ \rho^{\mathrm{O_2^-}}(x,t)\\ \rho^{\mathrm{O_3^-}}(x,t)\end{pmatrix} + \begin{pmatrix}w^{\mathrm{e}}(x,t)\\ w^{\mathrm{O_2^+}}(x,t)\\ w^{\mathrm{O^-}}(x,t)\\ w^{\mathrm{O_2^-}}(x,t)\\ w^{\mathrm{O_3^-}}(x,t)\end{pmatrix}\frac{\partial}{\partial x}\begin{pmatrix}\rho^{\mathrm{e}}(x,t)\\ \rho^{\mathrm{O_2^+}}(x,t)\\ \rho^{\mathrm{O^-}}(x,t)\\ \rho^{\mathrm{O_2^-}}(x,t)\\ \rho^{\mathrm{O_3^-}}(x,t)\end{pmatrix} =$$
$$\begin{pmatrix}\nu_{\mathrm{i}}-\nu_{\mathrm{a}}^{O}-\nu_{\mathrm{a}}^{O2} & 0 & \nu_{\mathrm{d}}^{O} & \nu_{\mathrm{d}}^{O2} & 0\\ \nu_{\mathrm{i}} & 0 & 0 & 0 & 0\\ \nu_{\mathrm{a}}^{O} & 0 & -\nu_{\mathrm{d}}^{O}-\nu_{\mathrm{c}}^{O3}-\nu_{\mathrm{c}}^{O2} & 0 & 0\\ \nu_{\mathrm{a}}^{O2} & 0 & \nu_{\mathrm{c}}^{O2} & -\nu_{\mathrm{d}}^{O2} & 0\\ 0 & 0 & \nu_{\mathrm{c}}^{O3} & 0 & 0\end{pmatrix}\begin{pmatrix}\rho^{\mathrm{e}}(x,t)\\ \rho^{\mathrm{O_2^+}}(x,t)\\ \rho^{\mathrm{O^-}}(x,t)\\ \rho^{\mathrm{O_2^-}}(x,t)\\ \rho^{\mathrm{O_3^-}}(x,t)\end{pmatrix} \tag{8}$$

We do not distinguish between flux and bulk velocity of species, since the difference is known to be quite small in the considered E/N range. The temporal evolution of species numbers, $n(t) = \int_{\mathrm{gap}} \rho\,(x,t)\,\mathrm{d}x$ is given as the exponential of matrix M:

$$\vec{n}\,(t+\mathrm{d}t) = e^{M\,\mathrm{d}t}\,\vec{n}\,(t), \tag{9}$$

which can be calculated numerically. The simulated displacement current is proportional to the velocity and density of the charge carriers in the entire gap:

$$I(t) \sim \sum_{j=1}^{N_{\mathrm{S}}}\sum_{i=1}^{N_{\mathrm{x}}} \rho^j(x_i,t)\,|w^j| \tag{10}$$

where N_{x} is the spatial discretisation of the electrode gap and the number of species N_{S}=5 in our model.

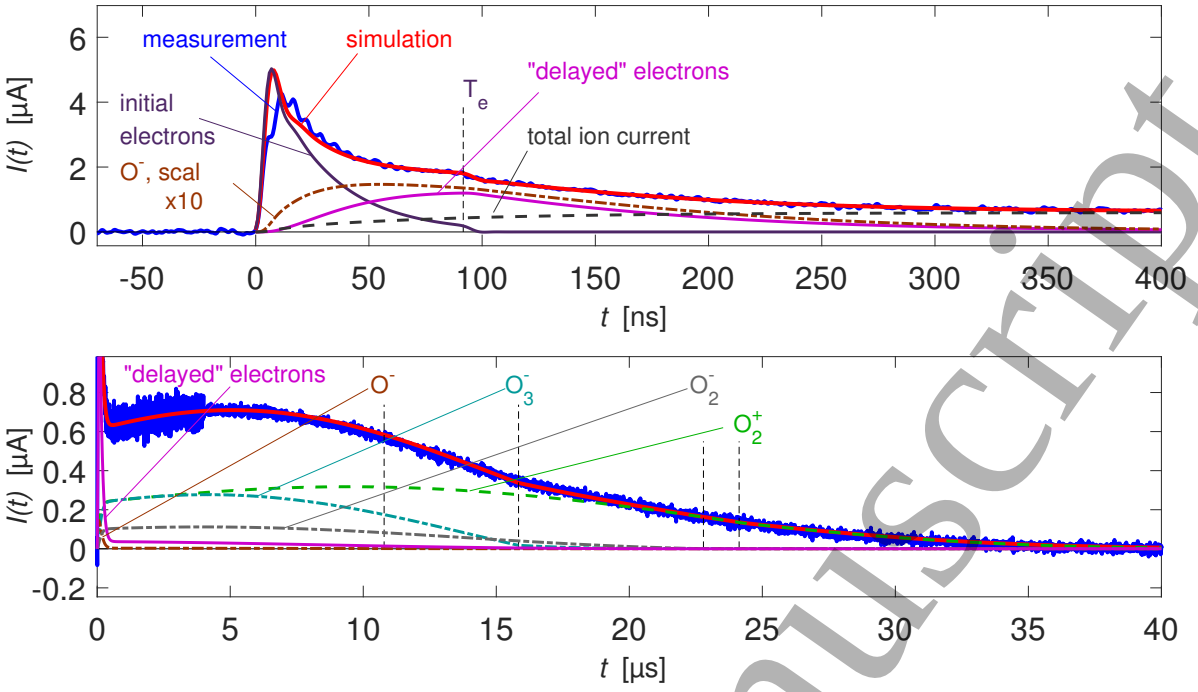

Figure 2: Measured current and simulation for a measurement at 40 kPa, mixture of 20% N_2 and 80% O_2 at 15 mm gap distance and E/N of 108 Td. The top graph shows the electron dominated part of the current of few hundred ns duration. The bottom graph shows the same signal, on a timescale of μs, for which ions clearly dominate the current shape. After 4 μs the current is low pass filtered for better visibility. The partial currents of different species resulting from the fitting process are shown. A substantial number of short-lived O^- ions are present only for a few 100 ns; their contribution is multiplied by a factor of 10 in the upper plot. The vertical lines correspond to the drift times of the species.

Figure 2 visualizes the measured current, and the partial currents of different species, as an output of the simulation. The signal is amplified and averaged over approximately 200 shots. After around 90 ns, the initially released electrons arrive at the anode. "Delayed electrons", i.e. electrons that have detached from either O^- or O_2^-, dominate until 300 ns. It is interesting to note that substantial current, caused by O_2^+, is present after the crossing time of positive ions (denoted as "O_2^+" in green in figure 2). This is possible in models with detaching electrons: the theoretical limit of the current is reached, when an electron attaches at $t = 0$, travels to the anode as a slow ion, detaches shortly before reaching the anode and ionizes a neutral molecule. Thus, a very small current is expected as late as the sum of the gap drift times of O_2^- and O_2^+. In our previous publication [19], we concluded that the mobility from reference publications was given too high, or that clusterization of positive ions takes place. However, this example shows that when using the full model, the simulated current fits perfectly the measurement, when using the referenced mobilities for O_2^+ from [34].

The model we chose is largely based on Pancheshnyi's work [17]. Most authors used a comparable, but not identical model:

- Neil, Craggs 1973 [8]: Similar to our model, yet without 3-body attachment rate to O_2^-, and an additional conversion rate from O_3^- to O^- (of considerable magnitude).
- Kinsman, Rees 1970 [12]: two different models are discussed, model 1 is referenced and is similar to our model, but does not include the O_2^- detachment rate (which we find to be rather small, but non-negligible). Three-body attachment to O_2^- is considered negligible (with which we agree). Like Neil and Craggs, an additional conversion rate from O_3^- to O^- is added in model 2.
- Sukhum, Prasad and Craggs 1967 [13]: Include ionization, attachment and O^- detachment in their model. They assume that different negative ions are predominant in different pressure ranges: O^- at low pressures (below 7 kPa) and O_2^- at high pressures above 13 kPa.
- Wagner 1971 [14]: includes ionization, attachment to O^-, O^- detachment and conversion from O^- to O_2^-. O_3^- is considered negligible, and O_2^- is assumed to be stable.
- Price, Lucas, Moruzzi 1973 [23]: Similar to our model, yet without 3-body attachment to O_2^- and without O_2^- detachment rate.
- Snuggs et al. 1971 [26] use a O^- ion source and investigates conversion rates to O_2^- and O_3^-.

In order to clarify the distinction between detachment of O^- and O_2^-, ν_d^O and ν_d^{O2}, we add a small amount of H_2 to pure oxygen. As has been pointed out by Moruzzi [35], the detachment of O^- is then greatly amplified by the exothermic process

$$O^- + H_2 \rightarrow H_2O + e^-. \tag{11}$$

The resulting rate coefficients for the measurements with small admixtures of hydrogen are likewise included in our result plots for comparison to pure O_2.

3.1. Critical field strength

Attaching gases, for which the attachment rate exceeds the ionization rate, exhibit a transition between exponential growth and decay of the number of free electrons over time. In many gases without complicated ion kinetic, the "effective rate" is easiest to measure, and simply defined as $\nu_\mathrm{eff} = \nu_\mathrm{i} - \nu_\mathrm{a}$. The so-called critical field strength $(E/N)_\mathrm{crit}$ is then the E/N value for which the ionization rate equals the attachment rate.

The model that we used in our previous publication, first presented by van der Laan and Verhaart [20], featured two negative ions ("stable" and "unstable"). Since the analytical solution is partially known, a suitable effective rate was defined by Wen and Wetzer [36], depending not only on ionization and attachment but also on detachment and conversion rates. We pointed out that this rate is the largest non-zero eigenvalue of the system

matrix, equation (8). For the model used in this publication with three negative ions, the analytical solution cannot easily be stated. Nevertheless, a necessary and sufficient condition for exponential growth of the densities is that at least one eigenvalue of the system matrix is larger than zero. We find that the "critical field" $(E/N)^*_{\mathrm{crit}}$, defined in such a way, is generally lower than the value for the "traditional" condition of equal electron attachment and ionization. Figure 13 in the results section shows both and illustrates the difference.

4. Fitting routine

We described the fitting routine in detail in a recent publication [19], including a convergence analysis of the simulation grid step size on GPUs. Starting with a random guess of rate coefficients within certain bounds, the fitting routine tries to find a set of rate coefficients $\vec{\nu}$ so that the simulation and measurement overlap best, i.e. minimize the norm ξ:

$$\xi(\vec{\nu}/N, \{r, E/N, d, p\}) = \int_{T_0}^{T} \left[s(\{r, E/N, d, p\}, t) - f(\vec{\nu}/N, t) \right]^2 \, \mathrm{d}t \tag{12}$$

where r is the relative content of oxygen, E/N is the reduced electric field strength, d is the electrode gap distance, p is the gas pressure, $s(t)$ is the measured current signal and $f(t)$ is the simulation. Through variation of the rates, an optimization routine tries to find an agreement between measurement and simulation.

In order to increase the informational content, and considering that measurements at different distances and equal E/N are described by the same set of rate coefficients, the optimization can work on a sum of norms $\Sigma_i \, \xi(r, E/N, d_i, p)$ for measurements at different gap distances $d_1 \ldots d_n$. This can even be taken a step further: assuming that all rates are either linear in pressure or quadratic in the case of the conversion rate (6) and three-body attachment rate (3), these measurements are subject to the same set of rate coefficients, which are pressure normalized by definition. Instead of fitting all measurements individually, we add up the norms for all measurements of equal E/N value (and equal gas mixture):

$$\tilde{\xi}(\vec{\nu}/N, \{r, E/N\}) = \sum_{i=1}^{n} \xi(\vec{\nu}/N, \{r, E/N, d_i, p_i\}) \tag{13}$$

We typically use $n = 10 - 40$ waveforms, where we diversify in the experimental settings of distance and pressure as far as possible, in order to maximize the informational content. The fitting routine thus tries to find a set of coefficients $\vec{\nu}/N$ ($\vec{\nu}/N^2$ in case of three-body rate coefficients), so that the sum of the objective function values $\tilde{\xi}$, equation (13), is minimal.

For this methods, the E/N value that we calculate from the vessel pressure, temperature and voltage measurement and distance, has to be sufficiently accurate: a set of measurements where a single measurement condition deviates only slightly (deviation

of sub percent in E/N), makes it impossible to find a "joint" solution for the whole set of measurements. The same holds true for measurements influenced by space charge effects.

5. Results

The following section presents the results of the fitting routine. For all seven rates a random starting point is created, within boundaries spanning two orders of magnitude. The found solution seems to be the global optimum, since we never encountered local optima, even when applying wider bounds for the starting point.
We found it necessary to preset electron and ion mobilities in order to reduce the number of fit parameters. The diffusion of electrons is preset but affects the measurements above 10 kPa only modestly. Ion diffusion is neglected.
The investigated N_2-O_2 mixtures contain 5, 10, 20, 40, 50, 60, 80, 90% of oxygen, as well as pure oxygen with and without traces of hydrogen. We experienced measurement difficulties (space charge effects and cathode efficiency) for partial pressures of oxygen above 60 kPa. For mixtures with less oxygen we measured from 3 kPa up to 100 kPa. The E/N range runs from 40 up to 120 Td where possible.
We obtain the electron diffusion and mobility with the method described in [37], at the lowest measured pressures (3 kPa, 6 kPa) at which ion kinetics plays only a minor role. We do not distinguish between bulk and flux velocity of electrons, a distinction which becomes important for discharges with high diffusion and ionization rates [38, 39]. For $N_2 : O_2$ mixtures below 120 Td the difference was estimated to less than 1% [39]. In figure 3 we compare the results to the mobilities calculated with MAGBOLTZ [40], as well as several included reference values [41, 42, 10, 2, 39, 15].
Our results for the density-reduced electron mobility follow the shape of the MAGBOLTZ calculation closely, but show a slight pressure dependency and are lower in value. Reference values of Urquijo et al. [2] for oxygen agree, with even lower electron mobility. The maximum deviation between our measurement and the MAGBOLTZ calculation is 3% for pure oxygen, and decreases towards mixtures with less oxygen.
In figure 4, the obtained diffusion coefficient is plotted against E/N. According to simulations, the influence of detachment on the current shape at these low pressures should be negligible when evaluating the diffusion, and hence, the use of the method presented in [37] is possible. For the fit, interpolated diffusion values are used.

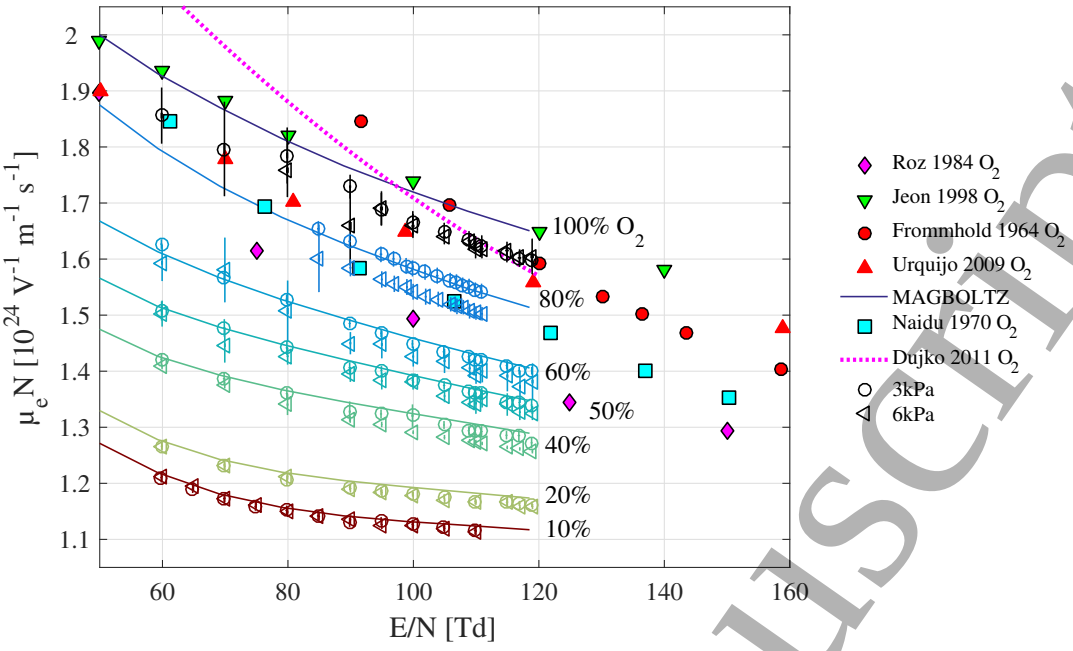

Figure 3: Density normalized electron mobility $\mu_e N$ as function of E/N, from low pressure measurements (3 kPa, 6 kPa) [37], MAGBOLTZ calculations and literature values for pure O_2 [41, 42, 10, 2, 15, 39].

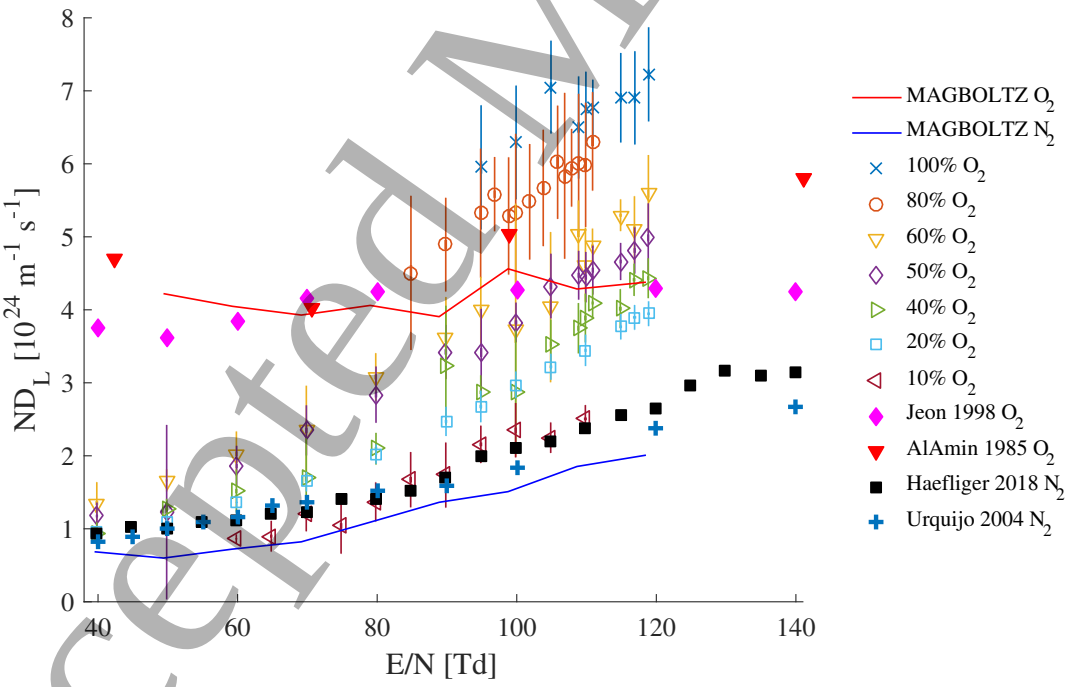

Figure 4: Density normalized longitudinal electron diffusion coefficient ND_L obtained with method [37] for the lowest measured pressures (3 kPa). The different concentrations are labeled and color coded. The references for O_2 are taken from [42, 43] and from [44, 21] for N_2.

As for the electron mobility, the ion mobilities for O^-, O_2^-, O_3^- and O_2^+ depend on the gas mixture. Literature values, which agree within a few percent, are available for pure oxygen and air [45, 46, 34]. We interpolate those linearly according to the mixing ratio and use them as simulation input.We checked the sensitivity of the fitted rates with regard to the ion mobilities for oxygen and found small differences of few percent, but no larger systematic shifts.

The ionization rate coefficient ν_i/N (fig. 5) is, according to the model, a superposition of the ionization of O_2 and N_2. It increases exponentially with E/N, and is higher for higher oxygen content of the gas mixture. There is a substantial spread in literature values for pure oxygen measurements, as depicted in fig. 5a. Our results are higher than measurements from Frommhold [9, 10] and lower than the results of the MAGBOLTZ [40] simulation. Our ionization rate agrees best with measurements from Moruzzi [11] and Kinsman [12]. For all N_2-O_2 mixtures, the trend agrees satisfyingly with the MAGBOLTZ results as depicted in figure 5b.

Figure 6 shows the dissociative attachment rate ν_a^O/N to O^-. This rate dominates over the three-body attachment rate to O_2^- at our measurement pressures (up to 100 kPa) and E/N values (higher than 40 Td). There is a rather large spread between the different measurements in pure oxygen by other authors [47, 7, 8, 23, 12, 48, 13, 14, 15, 16, 17, 39]. Our results mark the lower boundary of these measurements and fit best to the references of Moruzzi [23] and Kinsman [12]. Values of Dujko [39] are higher than our values (see figure 6b). While the results from the MAGBOLTZ calculation fit almost perfectly for gas-mixtures with a maximum of 60% oxygen content, they start to deviate for higher oxygen contents towards pure oxygen.

The three-body attachment rate coefficient ν_a^{O2}/N^2 to O_2^- (fig. 7) could not be obtained, and the values suggested by the fit show a large unsystematic scatter. The results roughly increase with increasing oxygen content, but do not show the expected physical decrease with increasing E/N. For several waveforms, the fitting results is identical with the lower boundary of the rate ($\approx 10^{-45}\,\mathrm{m^3 s^{-1}}$, not shown in the plot). Furthermore, only the results for mixtures with 50% mole fraction of oxygen and higher are plotted. Compared to the dominating dissociative attachment which forms O^-, the rate is seemingly too small to be derived reliably: in pure oxygen, for which three-body attachment is highest, and above 70 Td, direct formation of O_2^- accounts for less than 4 % of the total electron attachment according to Bolsig+ using values of 100 kPa. For the smallest measured E/N of $40\,Td$, the ratio is higher (≈10%), yet here the signal noise ratio of these measurements is rather weak. Disabling this process in the model yields equally good fits to the eye, and leaves the other rates mostly unchanged. The reason why for the measurements with traces of hydrogen higher values are found (which are still negligible compared to the dissociative attachment) is unclear; a physical cause is not necessarily compelling.

(a)

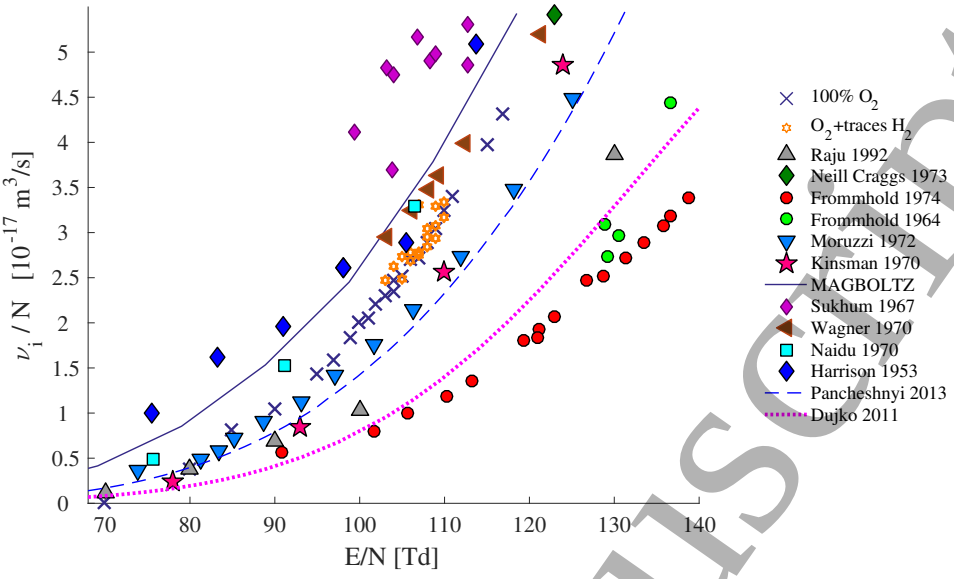

(b)

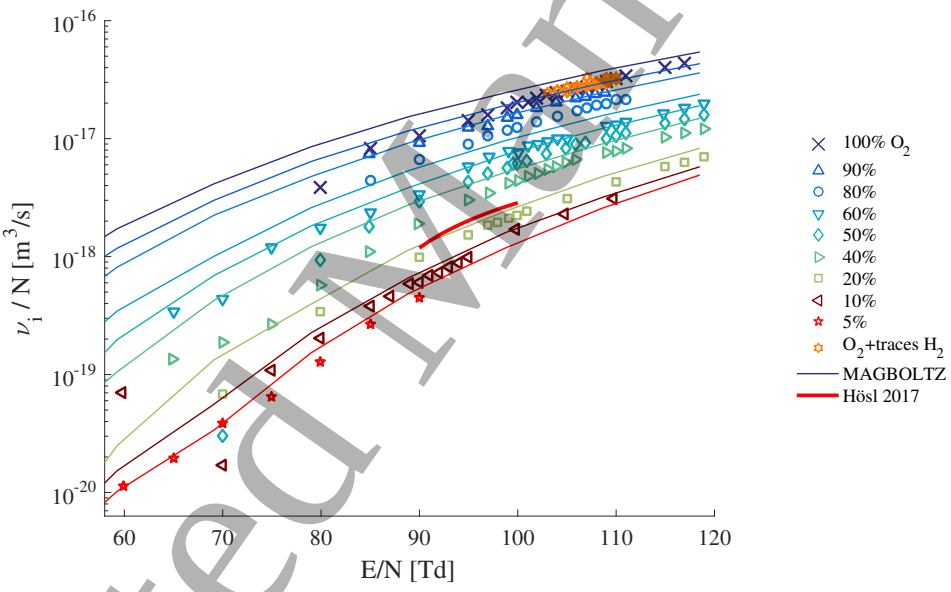

Figure 5: Ionization rate coefficient ν_i/N as a function of E/N (a) for pure oxygen and oxygen with traces of hydrogen is compared to literature data [7, 8, 9, 10, 11, 12, 13, 14, 15, 16, 17, 39] and MAGBOLTZ calculation [40]. (b) Different N_2-O_2 mixtures are shown, color and marker coded. The ionization rate coefficient of previous publication [19] (21% oxygen), where a simpler model was used, is included as reference.

Regardless of the fitting results, this rate might be non-negligible for the prediction of $(E/N)_{\mathrm{crit}}$ at several bar pressure, as can be seen in fig. 13. A detailed discussion of the three-body attachment process can be found in [50, 51]. Experimental data at lower E/N-values (up to 30 Td) is given in [52, 53], yet to our knowledge, no data is available

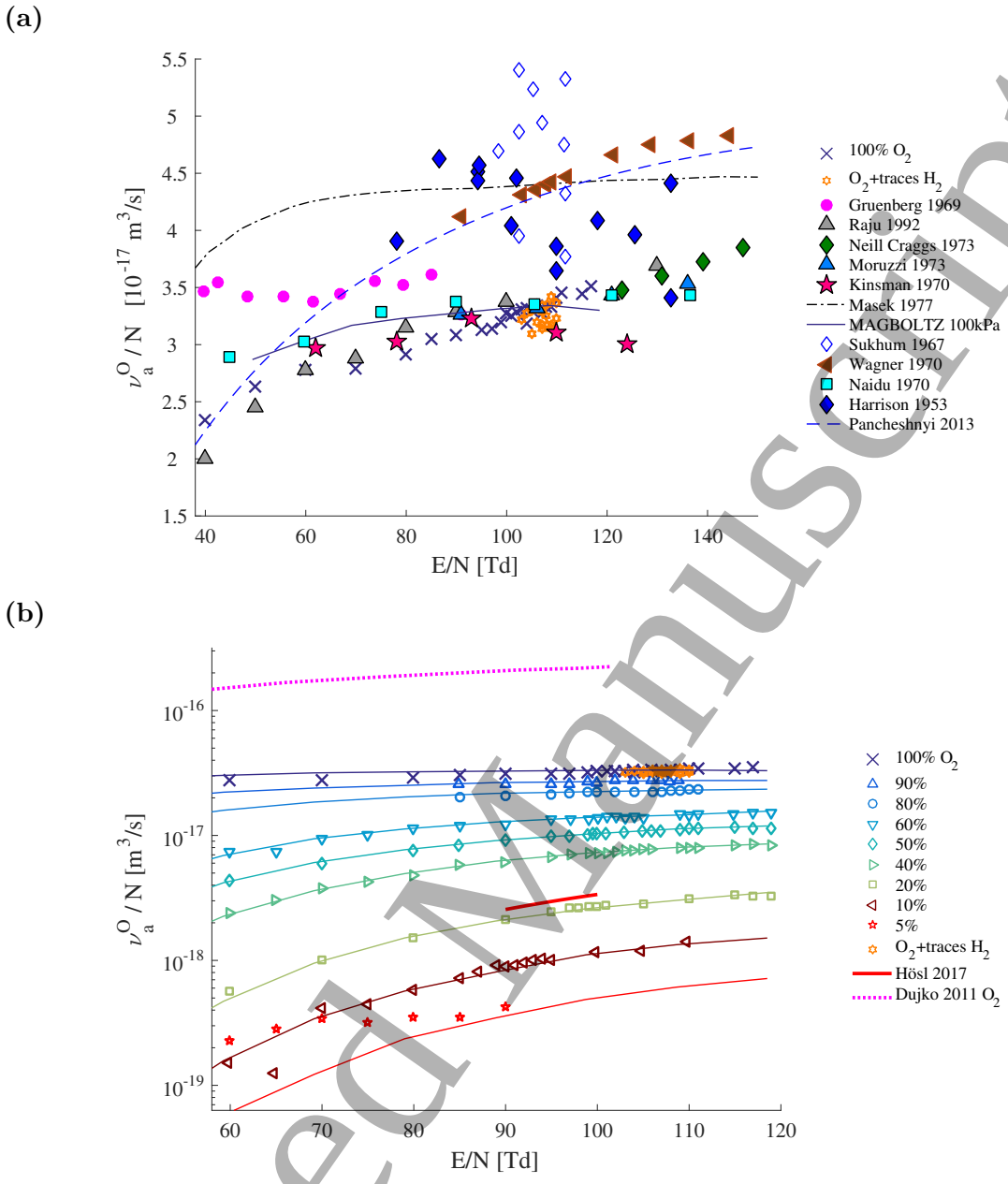

Figure 6: Dissociative attachment rate coefficient ν_a^O/N as a function of E/N (a) for pure oxygen and oxygen with traces of hydrogen is compared to literature data [47, 7, 8, 23, 12, 48, 13, 14, 15, 16, 17, 19] and MAGBOLTZ calculation [40]. (b) for different N_2-O_2 mixtures, color and marker coded. The dissociative attachment rate coefficient of Dujko for O_2 [39] and the previous publication [19] (21% oxygen), where a simpler model was used, is included as reference.

for higher E/N values. A theoretical curve is given in [39], focussing on lower E/N (through the logarithmic scale the emphasis is on values up to 20 Td), which is higher by an order of magnitude compared to the results of the Bolsig+ simulation around $(E/N)_{\mathrm{crit}}$.

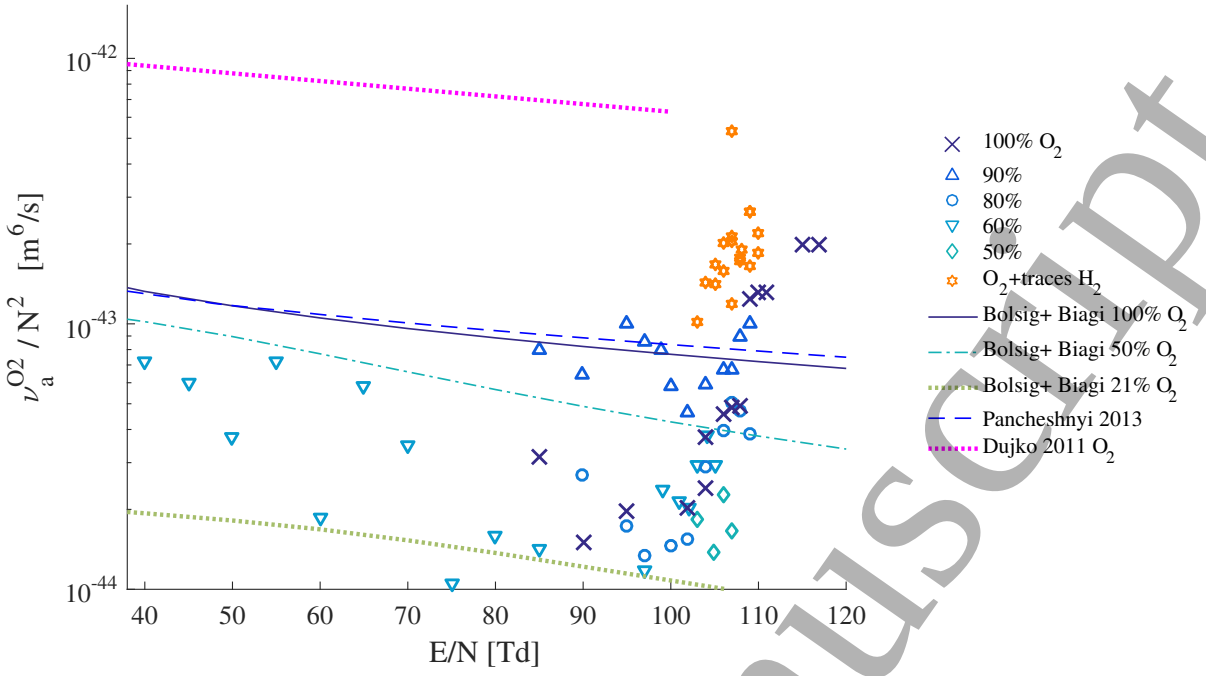

Figure 7: Three-body attachment rate coefficient ν_a^{O2}/N^2 in oxygen, theoretical calculations of [17, 39] and Bolsig+ [49] simulations using Biagi's cross section set from LXCat [45]. Dujko 2011 [39] was digitized from a double-logarithmic plot at the very end of the E/N range.

Figure 8 shows the O^- detachment rate coefficient ν_d^O/N. Our results fit with Frommhold (1964) [10], Neill and Craggs [8] and Sukhum [13], yet not with Kinsman [12], who obtained a lower value. Furthermore, we reference Frommhold 1974 [54], although Frommhold attributes the measured rate to O_2^-. The measurement in different gas mixtures in figure 8b shows that the rate is smallest for pure oxygen, and increases with increasing nitrogen content. The reference values from Moruzzi [56] for 1% O_2 does not show a E/N dependence similar to ours. The rates measured in oxygen with traces of hydrogen increase with hydrogen content and are further discussed in the discussion section.

In figure 9, showing the detachment rate coefficient ν_d^{O2}/N of O_2^-, disagreeing references are available from several authors [8, 54, 57, 58, 59, 17]. We plot only mixtures with oxygen concentration starting from 40%, since the higher number of O_2^- in the discharge is beneficial for estimating this rate. The measurement of Frommhold [54] was referenced in fig. 8 (the figure showing O^- detachment), where his values agree well with our ν_d^O/N. Comparing to our ν_d^{O2}/N, however, they are two orders of magnitudes higher. The findings of Neill and Craggs [8] for pure O_2 agree with only a slight offset. As Ponomarev and Aleksandrov [59] model is based on data from Frommhold [54], their theoretical results differ from ours by two orders of magnitude.

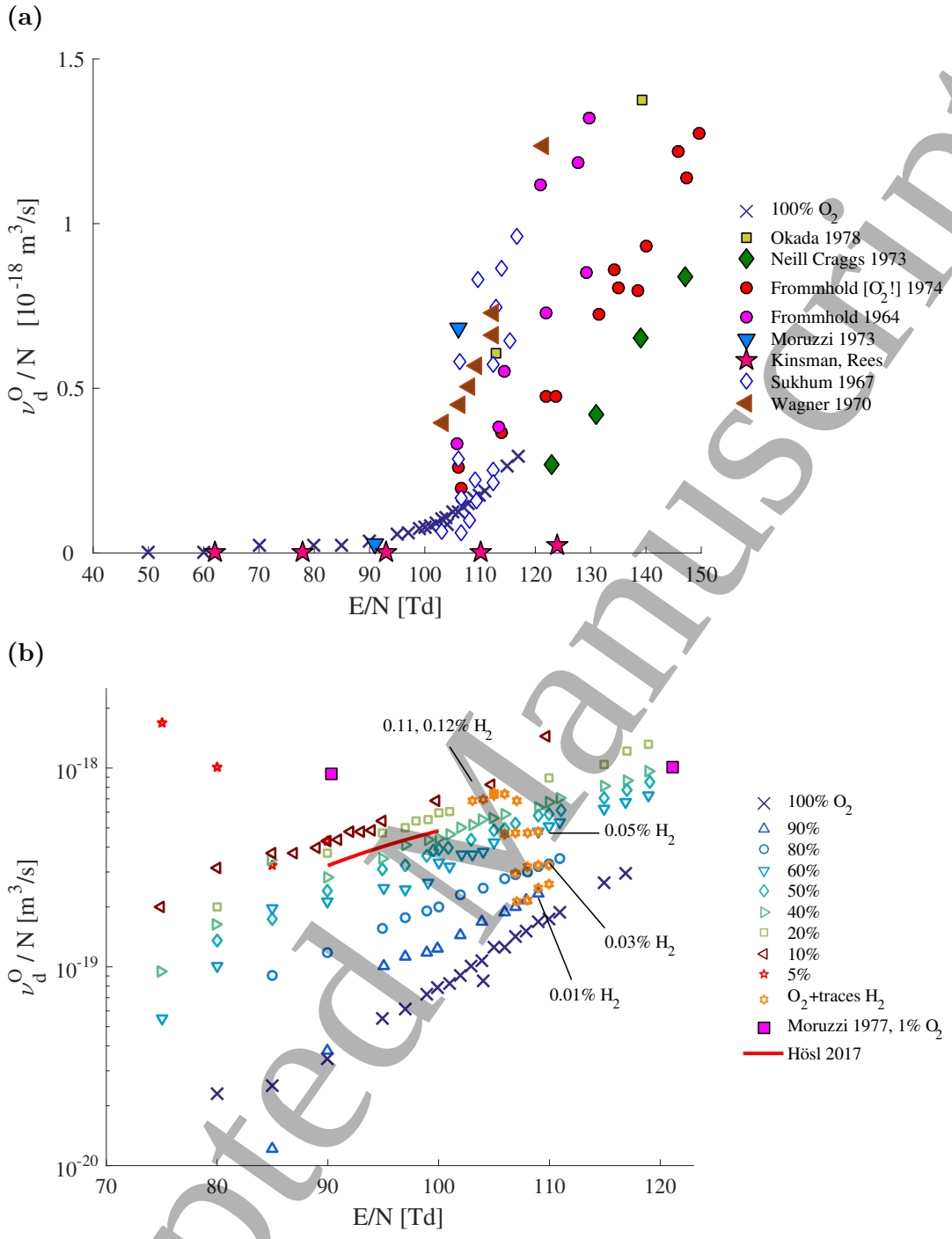

Figure 8: O^- detachment rate coefficient ν_d^O/N. (a) for pure oxygen, compared to reference data from [8, 54, 10, 23, 12, 13, 14, 55]. Frommhold's publication of 1974 is referenced, although he attributes the rate to O_2^- detachment. (b) for different oxygen content; for better visibility in log-scale. We compare to our older publication [19], and [56].

For the conversion rate coefficient $\nu_c^{O^3}/N^2$ in oxygen, results in figure 10a are compared

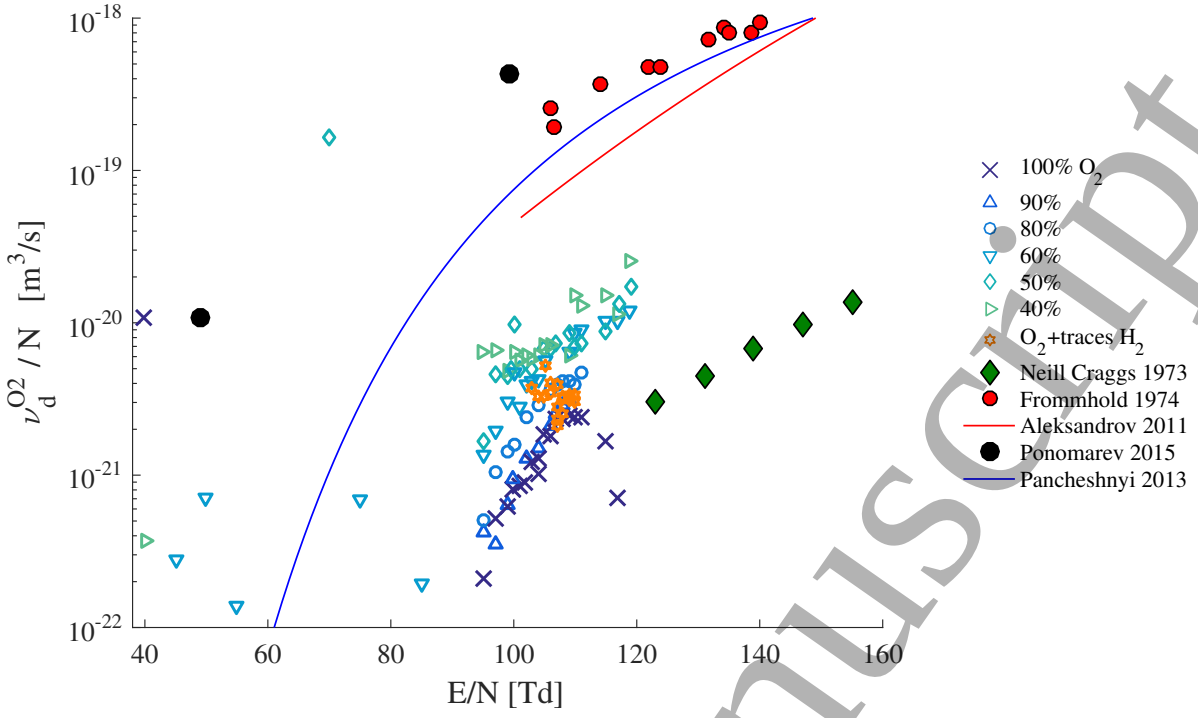

Figure 9: Detachment rate coefficient ν_d^{O2}/N of several gas mixtures with high oxygen content. References are taken from [8, 54, 57, 58, 59, 17].

to [8, 60, 24, 12, 17]. With the exception of Kinsman [12] the agreement is good below 100 Td, although our results are higher on average over the whole measurement range. The results below 80 Td are sensitive to shifts in on the chosen ion mobilities, which suggests a rather small confidence for the rate below 80 Td. For $E/N > 100$ Td, the theoretical calculation of Pancheshnyi [17] and the measurement of Neill and Craggs [8] disagree. Pancheshnyi calculates a decrease towards zero, while Neill and Craggs measure a constant value. Our results for lower oxygen concentration in figure 10b rather seem to support Pancheshnyi's findings, but are measured at low pressures due to being in the over-critical regime and lack the signal quality to decide for one or the other. Our previously obtained results [19] for 21% oxygen agree fairly well even though the fit model was simplified.

The ion conversion rate coefficient ν_c^{O2}/N describing O_2^- formation from O^- ions, process (5), is depicted in figure 11. A number of measurements are available for comparison [26, 8, 60, 12, 14, 17, 55]. As for most rates, our findings show the best agreement with the values of Neill and Craggs. The sensitivity with respect to small shifts in the ion mobility appears to be larger than for other rates. We estimate the confidence interval as roughly ±20% for the mixtures with sufficient oxygen content.

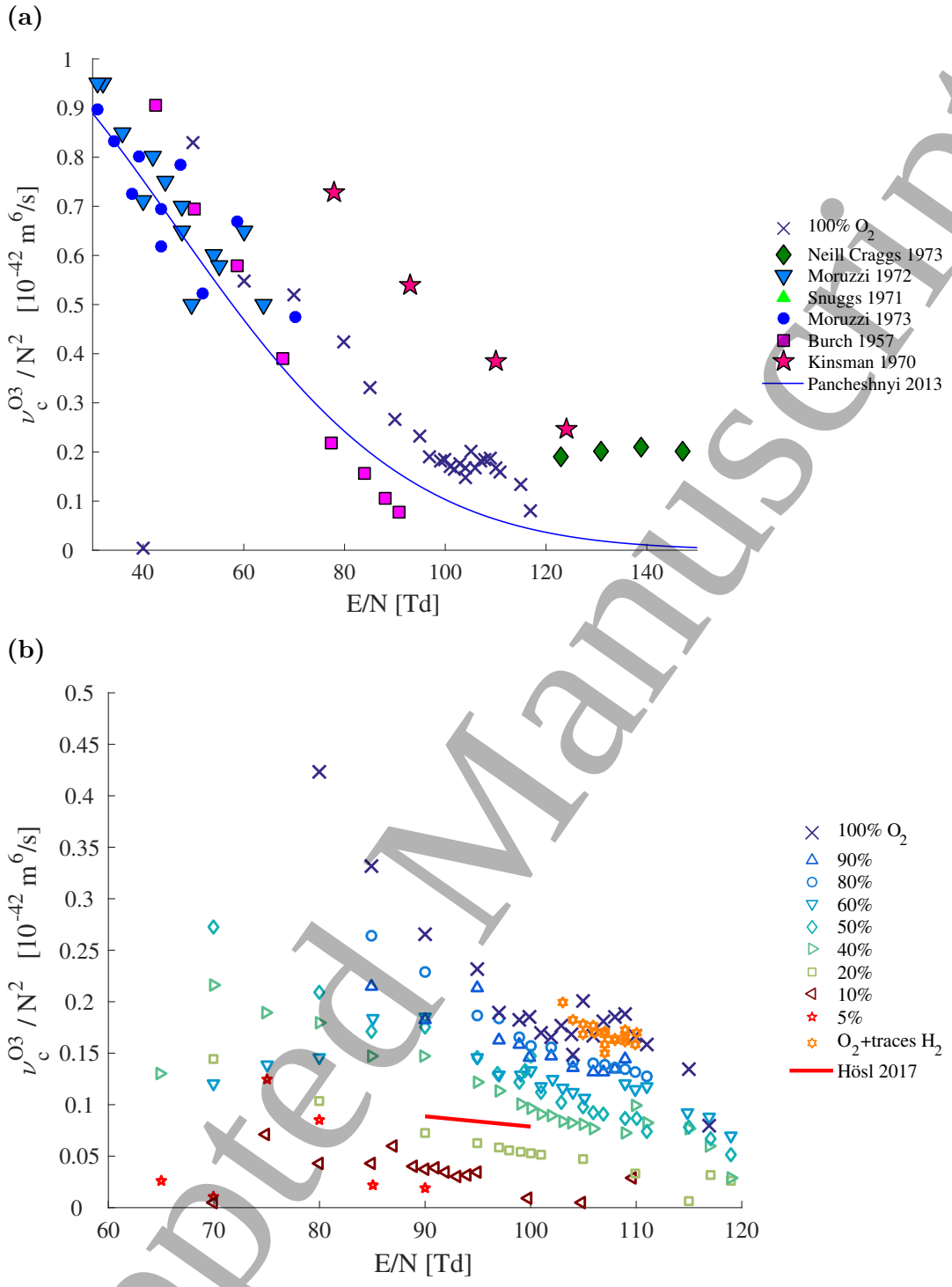

Figure 10: Conversion rate coefficient ν_c^{O3}/N^2 describing the formation of O_3^- from O^-. (a) compares literature data [8, 60, 24, 12, 17] to our results in pure oxygen. (b) compares different mixing ratios and includes our previous reference for dry air [19] (21% oxygen).

(a)

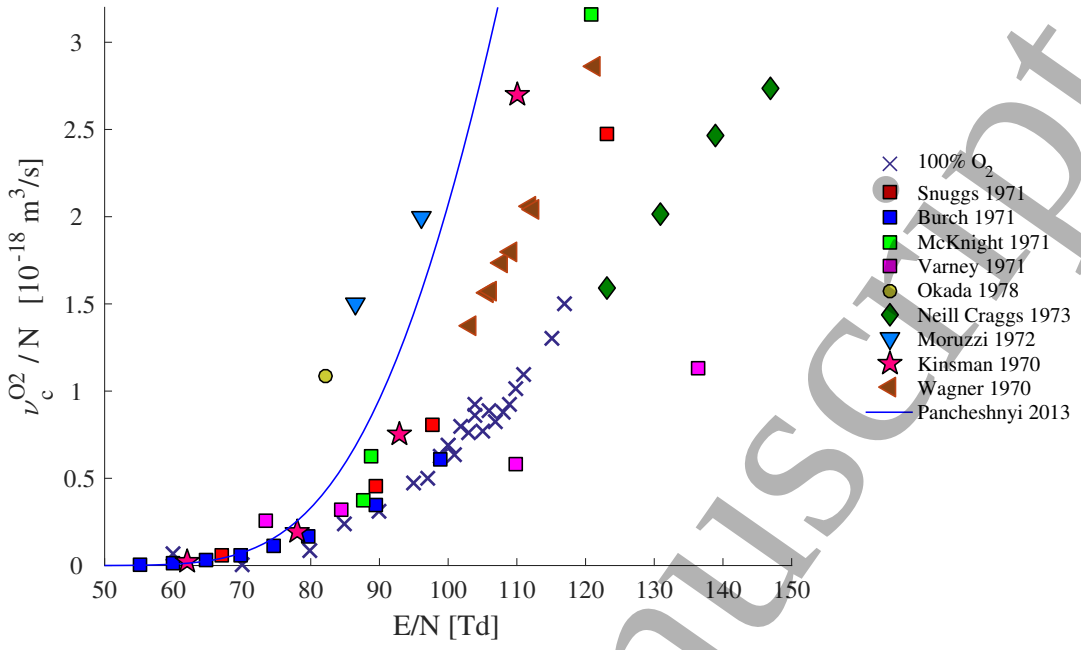

(b)

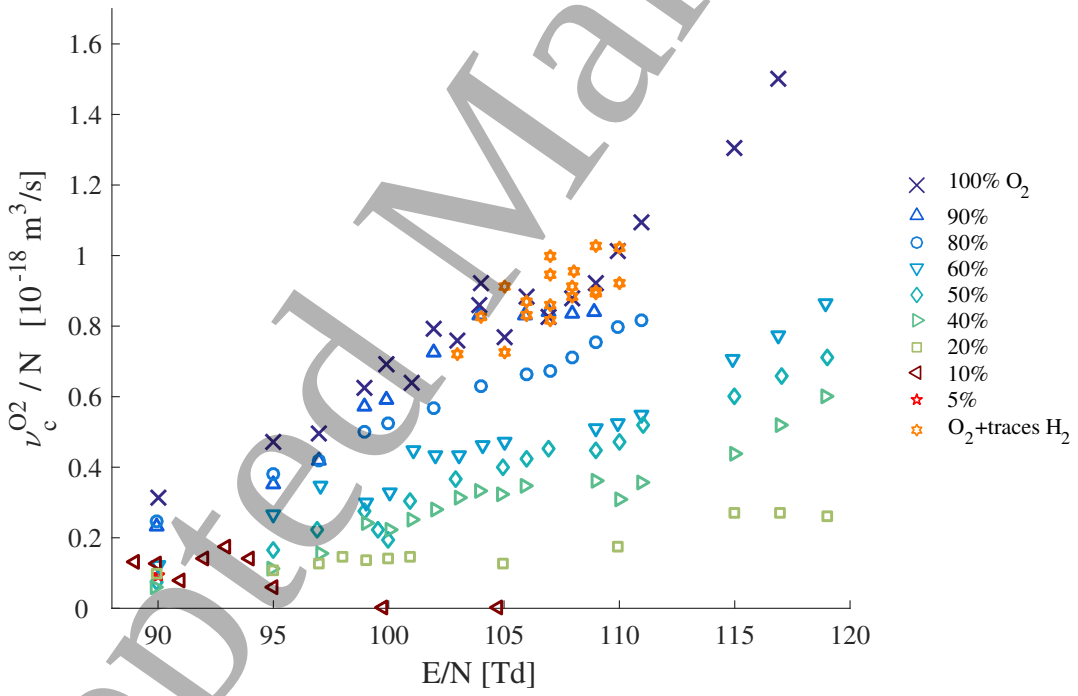

Figure 11: (a): Conversion rate coefficient ν_c^{O2}/N, describing the charge transfer from O^- to O_2^-, in pure oxygen is compared to literature values from [26, 8, 60, 12, 14, 17, 55]. (b) gives an overview of all measured gas-mixtures.

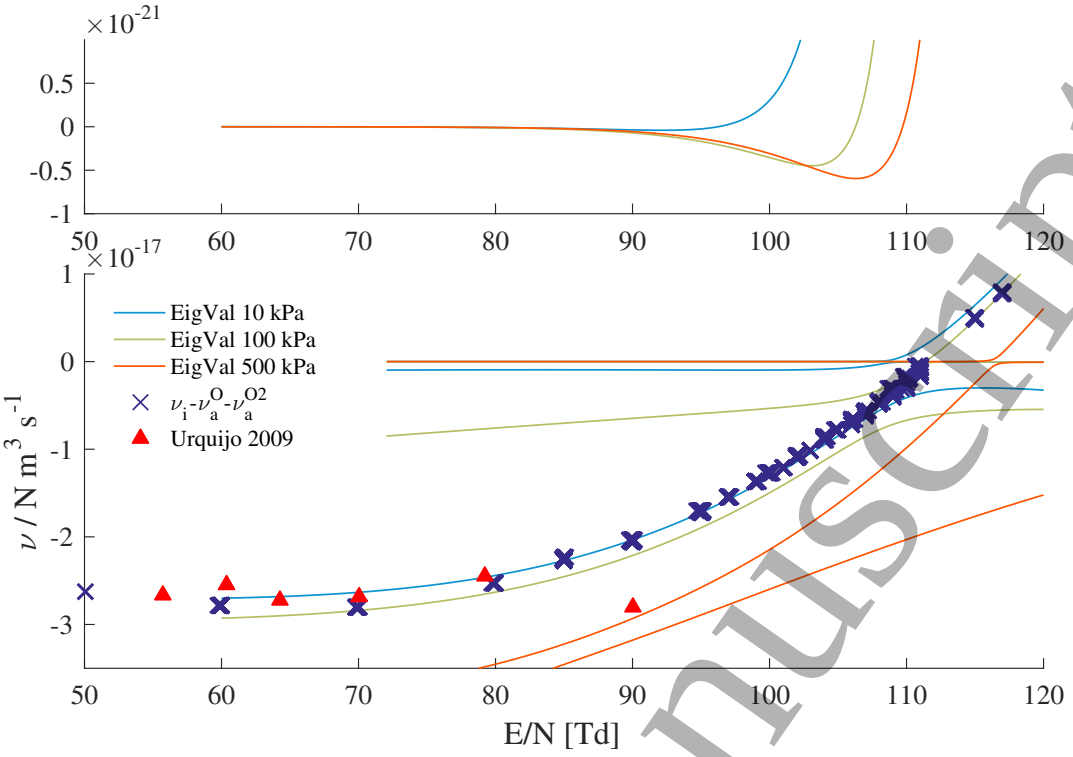

Figure 12: The three eigenvalues (from interpolation of the rates of the model) for 10, 100 and 500 kPa are plotted against E/N, and compared to the common definition of the effective rate coefficient ν_{eff}/N as $\nu_{\text{eff}}/N = (\nu_{\text{i}} - \nu_{\text{a}}^{O} - \nu_{\text{a}}^{O2})/N$ for pure oxygen (blue crosses). References are taken from [2]. The top plot zooms in on the zero crossing of the largest eigenvalue.

Figure 12 shows the three distinct (density-reduced) eigenvalues of the system matrix M, eq. (8), for pure oxygen. We interpolate the obtained rate coefficients (using the three-body attachment rate of MAGBOLTZ of figure 7) and evaluate the eigenvalues densely in E/N. The three-body rates ν_{a}^{O2} and ν_{c}^{O3} are scaled to 10, 100 and 500 kPa. For 500 kPa of pure oxygen, ν_{a}^{O2} becomes comparable to ν_{a}^{O} and thus non-negligible.
The smallest eigenvalue seemingly recovers the common definition of the effective rate coefficient, $\nu_{\text{eff}} = (\nu_{\text{i}} - \nu_{\text{a}}^{O} - \nu_{\text{a}}^{O2})/N$, as the comparison shows. The blue crosses depict ν_{eff}/N for pure oxygen and arbitrary pressure. The zero-crossing at 111 Td defines "$(E/N)_{\text{crit}}$" as $(\nu_{\text{i}} - \nu_{\text{a}}^{O} - \nu_{\text{a}}^{O2})/N = 0$. The effective rate coefficient can be regarded as describing the evolution of the electrons in the head of the avalanche, regardless of detachment effects, which influence only the tail. Comparing to $(E/N)_{\text{crit}}$ of [2], we find good agreement for the E/N range below 90 Td.
The largest eigenvalue, on the other hand, approaches zero from below for decreasing E/N, and becomes positive at 95, 105 and 108 Td for the respective pressures (top plot of figure 12). This transition defines $(E/N)^{*}_{\text{crit}}$, which we propose as alternative criteria for the critical field strength. The eigenvalue remains positive yet small in the interval between $(E/N)^{*}_{\text{crit}}$ and $(E/N)_{\text{crit}}$ (not visible in the figure).

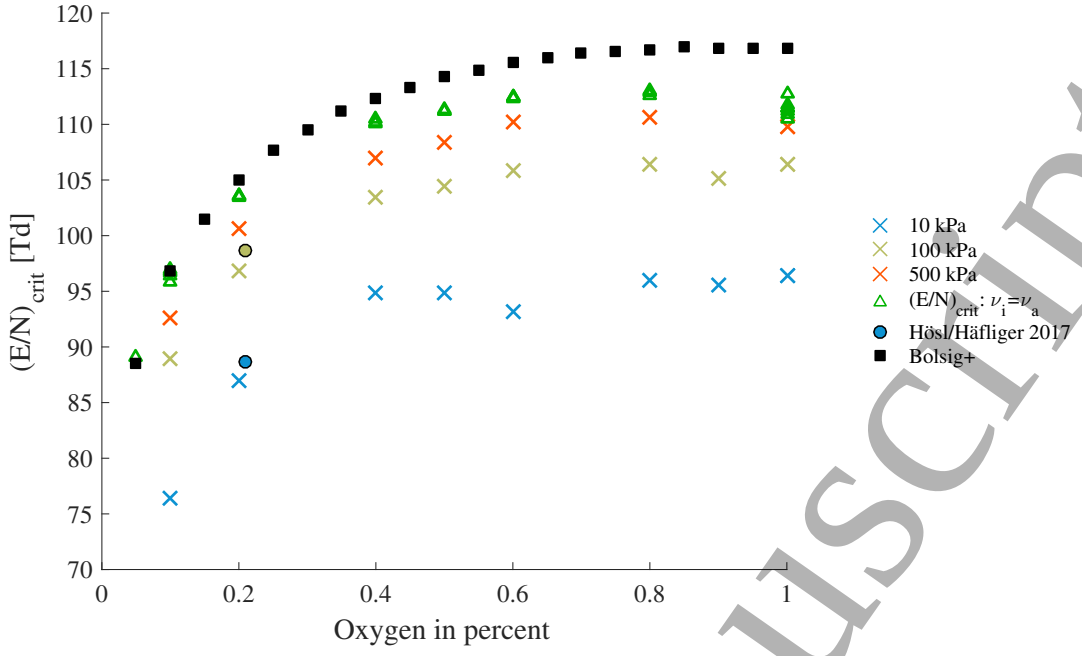

Figure 13: Critical electrical field $(E/N)^*_{\mathrm{crit}}$ for 10, 100 and 500 kPa in pure O_2. Compared to the common definition of $(E/N)_{\mathrm{crit}}$, plotted in green for various pressures, the $(E/N)^*_{\mathrm{crit}}$ values are lower. The $(E/N)^*_{\mathrm{crit}}$ of [19] agrees for synthetic air, while the $(E/N)_{\mathrm{crit}}$ of a Bolsig+ calculation [49, 40] (Biagi cross section set) are higher.

Using these two definitions, two values for the density-reduced critical electric field are obtained. The $(E/N)^*_{\mathrm{crit}}$ in figure 13 (blue, yellow, red crosses) increase with higher pressure and oxygen concentration. The findings agree with our previous publication [19], where we used an analytical formula for $(E/N)^*_{\mathrm{crit}}$ values for synthetic air. $(E/N)_{\mathrm{crit}}$, derived using only attachment and ionization (green symbols), is higher for all gas-mixtures. The $(E/N)_{\mathrm{crit}}$ of a Bolsig+ simulation [49] (Biagi's cross section set [40]) agrees for mixtures with high content of nitrogen, while deviating slightly for higher oxygen concentrations.

6. Discussion

Our fitting routine relies foremost on the experimental accuracy in E/N, since one set of rate coefficients is fitted for multiple waveforms of different distance and pressure. Great care has been taken to achieve an overall error smaller than $\pm 0.5\%$ in E/N [21] in our experiment. The reduction in the spread, compared to our older attempt [19], is due to the combination of increased experimental accuracy and the increase in informational content through using different distances and pressures as input for the fitting routine. We were able to almost double the number of fit parameters, while sustaining a small spread for most rate coefficients.

Overall, our results agree well with most references, with the exception of the detach-

ment rate of O_2^-. It is difficult to assess the sensitivity of the individual rate coefficients: the fitting spread gives an impression, but might not reflect systematic errors. For example, the dissociative attachment rate coefficient ν_a^O/N seems to be perfectly aligned with the MAGBOLTZ simulation for oxygen content lower than 60%. Above, the steepness is different, with a rather small spread, in alignment with referenced values from Liu, Raju [7] and Neil, Craggs [8]. However, acceptable fits to the eye are likewise achieved if the MAGBOLTZ results for ν_a^O/N are used. An effective confidence interval is difficult to assign, but is certainly larger than the visible spread, which is not surprising since 7 rates are fitted simultaneously.

In order to present a more complete set of swarm parameters, the electron mobility and diffusion coefficient are included. These results, however, were obtained using a different evaluation method [37]. Without presetting these parameters, the necessary fit time increases drastically. The obtained electron mobility and used literature ion mobilities match well with the measurements. This was ensured by comparing the simulation and measured current as shown in fig. 2. The agreement of the drift velocities between simulation and measured current is, throughout the whole measurement series, satisfying to the eye.
The measured ionization rate coefficient lies in between several references, and increases with increasing relative oxygen content. We find lower values than predicted by the MAGBOLTZ simulation for all mixtures. The spread in the reference values is rather large, which is explained by the difficulty of measuring and modelling O_2.

We were not able to deduce the three-body attachment rate ν_a^{O2}, due to the rate being two orders of magnitude smaller than the dominating dissociative attachment ν_a^O in the considered E/N and pressure range. Increasing the measurement pressure (above 60 kPa) in pure oxygen further would help in accessing the rate. We were, however, unable to do so since these measurements are increasingly difficult: in order to avoid space charge effects, it is necessary to limit the number of charge carriers in the electrode gap by attenuating the laser power. Hence, the signal to noise ratio decreases. Averaging over more samples would require a photocathode which does not decrease in efficiency.

The detachment rate coefficient ν_d^O/N for O^- in oxygen is well within the spread of the references to the results of [8, 54, 10, 23, 12, 13]. Kinsman, Rees [12] derive a lower value, when we take their "reaction scheme 1" which fits our model. Comparing different gas mixtures, we find that ν_d^O/N increases with increasing nitrogen content. This fits the physical picture: through the process of eq. (4) the electron efficiently detaches [56]. In fig. 8a we included two references of Frommhold from 1964 [10] and 1974 [54]. Both seem to fit well, however, the rate coefficient in the latter is attributed to the detachment of O_2^-. In both publications it is clearly stated that the detachment of O^- is thought to be the higher rate, and detachment of O_2^- to be comparably slow, which matches our findings. Yet, Frommhold seems to arrive at the conclusion that his

earlier assessment is wrong, with which we disagree. The reference from 1974 [54] is plotted for comparison additionally in figure 9. Our value for ν_d^{O2}/N seems to match the one of Neill and Craggs [8], yet contrasts strongly with that of Frommhold [54]. The theoretical values of Pancheshnyi [17] and Ponomarev and Aleksandrov [59] are based on Frommhold's results, which they use as input for their models. Ponomarev and Aleksandrov [59] discuss the discrepancy in between those two measurements [54, 8] and judge the results of Frommhold more reliable, which they use as input for their further calculation.

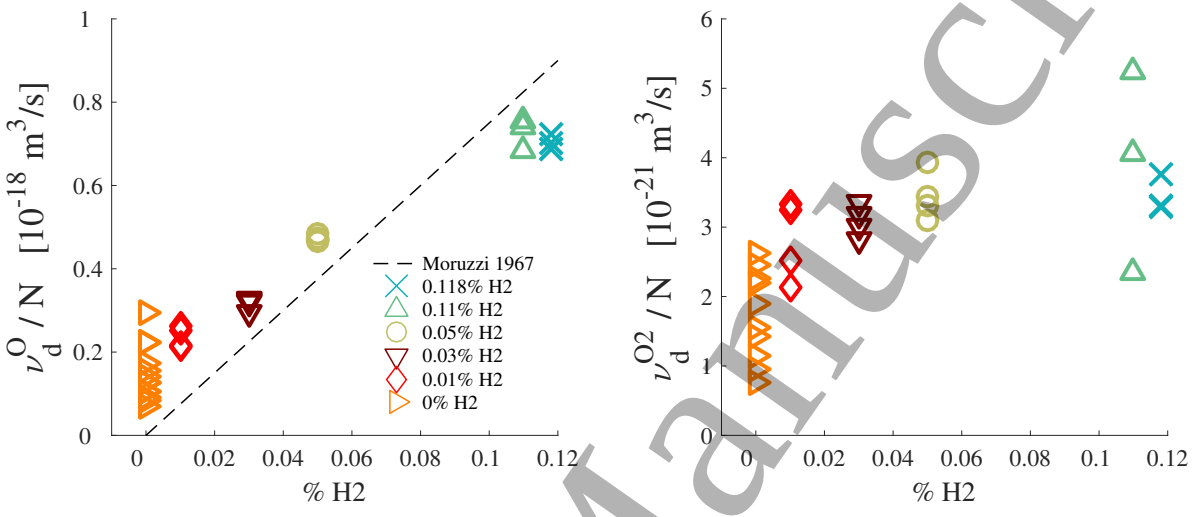

Figure 14: Left plot: Results for the detachment rate coefficient of O^- according to process $O^- + H_2 \rightarrow H_2O + e$, equation (11), in the range of 100-110 Td, measured in $H_2 - O_2$-mixtures and compared to a reference from Moruzzi [35].

In order to clarify the distinction between ν_d^O and ν_d^{O2}, we add a small amount of H_2 to pure oxygen. Moruzzi finds a value of $k = 7.5 \cdot 10^{-16}\,\mathrm{m^3 s^{-1}}$ for the detachment O^- via $O^- + H_2 \rightarrow H_2O + e$, where k is normalized to 100% hydrogen content, measured at 60 Td and lower. He further finds no apparent E/N dependence, as is expected from a strongly exothermic process. To our knowledge, there is no similar detachment process for O_2^- with hydrogen.

The left side of fig. 14 shows the O^- detachment rate ν_d^O/N increasing with increasing H_2 content. A factor of 5 lies between a measurement from $E/N = 100-110$ with 0.1% of H_2 in O_2, compared to pure oxygen. We find a linear dependence of the rate on the H_2 concentration, with an offset of roughly $1 \cdot 10^{-19}\,\mathrm{m^3 s^{-1}}$, fitting well with Moruzzi's results.

The results for the O_2^- detachment rate, shown on the right side of fig. 14, shows a lower relative and absolute increase, and remain three orders of magnitude smaller. Other rates stay mostly unchanged when adding H_2, as can be seen in the result plots.

We consider this as confirmation that the fit can indeed distinguish the different ions, and that both rates can be reliably differentiated. Our measurements therefore confirm the results of Neil and Craggs [8].

This leaves the question whether the discrepancy might come from a confusion of O_2^- and O_4^- ions. Frommhold [54] and Kinsman [12], using a mass spectrometer, report that almost no O_4^- was observed at the critical field strength. Urquijo, on the other hand, measuring at much lower electric fields, reports that mostly O_4^- is present in the gap for a measurement below 20 Td. The mobility of O_4^- is unknown at the critical field strength, and we can therefore not decide between the two species, and refer to the ion as O_2^- for simplicity, and because it matches the reported mobility of O_2^-.
For ν_d^{O2}/N, the detachment rate coefficient of O_2^-, we find an increase with increasing relative nitrogen content. This is surprising since Kossyi [29] states that the rate coefficient for O_2^- detachment upon collision with nitrogen is two orders of magnitudes less efficient than upon collision with neutral oxygen, with the possible exception of electronically excited N_2. We discussed neutral excited species in our last publications [19, 21] and assume that only very few species are created.
The results for the conversion rate coefficient ν_c^{O3}/N, corresponding to the process $O^- + O_2 + M \rightarrow O_3^- + M$ of eq. (6), are consistent with literature values. Neill and Craggs [8] measure a seemingly constant conversion rate above 120 Td, while the calculation of Pancheshnyi [17] decreases towards zero. Our measurements seem to follow the trend of Pancheshnyi, but have to be regarded with caution. Measurements above 110 Td have to be performed at low pressures due to the exponential growth of electrons. Therefore, their sensitivity to the three-body conversion rate is rather low.
The conversion rate coefficient ν_c^{O2}/N for the process $O^- + O_2 \rightarrow O_2^- + O$, eq. (5), fits again well with the references, and especially with Neill and Craggs [8]. The rate increases with both increasing E/N and higher oxygen content, since it is an endothermic process: the electric strength of the binding is higher for elemental oxygen (≈ 1.5 eV) [61] compared to O_2^- (≈ 0.5 eV) [62].

We evaluated the critical electric field according to two different definitions. Our proposed, alternative criteria takes into account the various detachment and conversion processes and yields a lower, pressure-dependent value. In the limit of high pressure, both values are identical. The reason for this is that at high pressure the three-body conversion rate to O_3^-, which competes with (two-body) detachment of O^-, becomes dominant. Most O^- is then converted to O_3^-, and the influence of detachment processes diminishes. This results are in agreement to our last publication, where the evaluation was done based on an analytic expression from a simpler model.
For the results for 500 kPa pure oxygen we took the three-body attachment rate calculated in MAGBOLTZ, and scaled it accordingly with pressure. Although the process is relatively weak at the critical field strength, it makes up for roughly 25% of the total attachment and is thus not negligible.

7. Conclusion

Using a model with four ion species and seven rate coefficients, we were able to satisfyingly fit N_2-O_2 measurements for a wide range of pressures, electric field and gas-mixtures. We compare our results to a variety of references and find good agreement for most rate coefficients. An additional measurement with a small admixture of hydrogen serves as a consistency check of the model, and shows that the informational content of the waveforms is sufficient to distinguish between the two detaching ions, O^- and O_2^-. The presented method can be a useful tool for the analysis of other gases or mixtures exhibiting electron detachment and ion conversion. For instance, the gas N_2O is known to be largly influenced by electron detachment. For estimating the critical electric field strength of the mixtures we propose a criterion based on the eigenvalues of the matrix describing the interaction of electrons and ions, equation (8). The resulting $(E/N)^*_{\mathrm{crit}}$ is pressure dependent and implicitly takes electron detachment into account.

Acknowledgments

This work is financially supported by GE Grid (Switzerland) GmbH, Pfiffner Technologie AG, ABB Switzerland and Siemens AG.

References

[1] M Capitelli, C M Ferreira, B F Gordiets, and A I Osipov. *Plasma kinetics in atmospheric gases*, volume 31. Springer Science & Business Media, 2013.

[2] M Yousfi, J de Urquijo, A Juarez, E Basurto, and J L Hernandez-Avila. Electron swarm coefficients in CO_2-N_2 and CO_2-O_2 mixtures. *IEEE Transactions on Plasma Science*, 37(6):764–772, 2009.

[3] L Niemeyer. A systematic search for insulation gases and their environmental evaluation. In *Gaseous Dielectrics VIII*, pages 459–464. Springer, 1998.

[4] M Rabie and C M Franck. Computational screening of new high voltage insulation gases with low global warming potential. *IEEE Transactions on Dielectrics and Electrical Insulation*, 22(1):296–302, 2015.

[5] Y Kieffel. Characteristics of g3 -an alternative to SF_6. In *Dielectrics (ICD), 2016 IEEE International Conference on*, volume 2, pages 880–884. IEEE, 2016.

[6] Rokunohe et al. Development of 72kv high-pressure air-insulated gis with vacuum circuit breaker. *Electrical Engineering in Japan*, 157:1270–1278, 2006.

[7] J Liu and G R Raju. Calculation of electron swarm parameters in oxygen using a rigorous Boltzmann equation analysis. *Canadian journal of physics*, 70(4):216–224, 1992.

[8] B C O'Neill and J D Craggs. Collisional detachment of electrons and ion molecule reactions in oxygen. *Journal of Physics B: Atomic and Molecular Physics*, 6(12):2625, 1973.

[9] R J Corbin and L Frommhold. Electron avalanches in oxygen and in mixtures of O_2 and H_2: determination of the first Townsend coefficient α. *Physical Review A*, 10(6):2273, 1974.

[10] L Frommhold. Über verzögerte Elektronen in Elektronenlawinen, insbesondere in Sauerstoff und Luft, durch Bildung und Zerfall negativer Ionen (O^-). *Fortschritte der Physik*, 12(11):597–642, 1964.

[11] D A Price, J Lucas, and J L Moruzzi. Ionization in oxygen-hydrogen mixtures. *Journal of Physics D: Applied Physics*, 5(7):1249, 1972.

[12] P R Kinsman and J A Rees. Ionization, attachment and ionmolecule reactions in oxygen. *International Journal of Mass Spectrometry and Ion Physics*, 5(1-2):71–81, 1970.

[13] N Sukhum, A N Prasad, and J D Craggs. Electron attachment and detachment in oxygen. *British Journal of Applied Physics*, 18(6):785, 1967.

[14] K H Wagner. Ionization, electron-attachment,-detachment, and charge-transfer in oxygen and air. *Zeitschrift für Physik*, 241(3):258–270, 1971.

[15] M S Naidu and A N Prasad. Mobility, diffusion and attachment of electrons in oxygen. *Journal of Physics D: Applied Physics*, 3(6):957, 1970.

[16] M A Harrison and R Geballe. Simultaneous measurement of ionization and attachment coefficients. *Physical Review*, 91(1):1, 1953.

[17] S Pancheshnyi. Effective ionization rate in nitrogen–oxygen mixtures. *Journal of Physics D: Applied Physics*, 46(15):155201, 2013.

[18] H Zhao and H Lin. Dielectric breakdown properties of N_2-O_2 mixtures by considering electron detachments from negative ions. *Physics of Plasmas*, 23(7):073505, 2016.

[19] A Hoesl, P Haefliger, and C M Franck. Measurement of ionization, attachment, detachment and charge transfer rate coefficients in dry air around the critical electric field. *Journal of Physics D: Applied Physics*, 50(48):485207, 2017.

[20] H F A Verhaart and P C T Van der Laan. The influence of water vapor on avalanches in air. *Journal of applied physics*, 55(9):3286–3292, 1984.

[21] P Haefliger and Franck C M. Detailed precision and accuracy analysis of swarm parameters from a pulsed townsend experiment. *Review of Scientific instruments*, 89(2):023114, 2018.

[22] L Frommhold, R J Corbin, and D W Goodson. Electron avalanches in oxygen: Theory. *Physical Review A*, 8(3):1403, 1973.

[23] D A Price, J Lucas, and J L Moruzzi. Current growth in oxygen. *Journal of Physics D: Applied Physics*, 6(12):1514, 1973.

[24] D A Parkes. Negative-ion/molecule reactions under swarm conditions. *Vacuum*, 24(11-12):561–571, 1974.

[25] L G McKnight. Drift velocities and interactions of negative ions in oxygen. *Physical Review A*, 2(3):762, 1970.

[26] R M Snuggs, D J Volz, I R Gatland, J H Schummers, D W Martin, and E W McDaniel. Ion-molecule reactions between O^- and O_2 at thermal energies and above. *Physical Review A*, 3(1):487, 1971.

[27] Y Itikawa. Cross sections for electron collisions with nitrogen molecules. *Journal of physical and chemical reference data*, 35(1):31–53, 2006.

[28] Y Itikawa. Cross sections for electron collisions with oxygen molecules. *Journal of Physical and Chemical Reference Data*, 38(1):1–20, 2009.

[29] I A Kossyi, A Y Kostinsky, A A Matveyev, and V P Silakov. Kinetic scheme of the non-equilibrium discharge in nitrogen-oxygen mixtures. *Plasma Sources Science and Technology*, 1(3):207, 1992.

[30] D Smith, N G Adams, and T M Miller. A laboratory study of the reactions of N^+, N_2^+, N_3^+, N_4^+, O^+, O_2^+, and NO^+ ions with several molecules at 300 k. *The Journal of Chemical Physics*, 69(1):308–318, 1978.

[31] A Bekstein, M Benhenni, M Yousfi, O Ducasse, and O Eichwald. Ion swarm data of N_4^+ in N_2, O_2 and dry air for streamer dynamics simulation. *The European Physical Journal Applied Physics*, 42(1):33–40, 2008.

[32] A Bekstein, M Yousfi, M Benhenni, O Ducasse, and O Eichwald. Drift and reactions of positive tetratomic ions in dry, atmospheric air: Their effects on the dynamics of primary and secondary streamers. *Journal of Applied Physics*, 107(10):103308, 2010.

[33] J de Urquijo, A Bekstein, O Ducasse, G Ruíz-Vargas, M Yousfi, and M Benhenni. Negative ion clusters in oxygen: collision cross sections and transport coefficients. *The European Physical Journal D*, 55(3):637–643, 2009.

[34] H W Ellis, R Y Pai, E W McDaniel, E A Mason, and L A Viehland. Transport properties of gaseous ions over a wide energy range. *Atomic Data and Nuclear Data Tables*, 17(3):177–210, 1976.

[35] J L Moruzzi, J W Ekin Jr, and A V Phelps. Electron production by associative detachment of O^--ions with NO, CO, and H_2. *The Journal of Chemical Physics*, 48(7):3070–3076, 1968.

[36] C Wen and J M Wetzer. Electron avalanches influenced by detachment and conversion processes. *Electrical Insulation, IEEE Transactions on*, 23(6):999–1008, 1988.

[37] A Chachereau, M Rabie, and C M Franck. Electron swarm parameters of the hydrofluoroolefine HFO1234ze. *Plasma Sources Science and Technology*, 25(4):045005, 2016.

[38] I Korolov, M Vass, N Kh Bastykova, and Z Donkó. A scanning drift tube apparatus for spatiotemporal mapping of electron swarms. *Review of Scientific Instruments*, 87(6):063102, 2016.

[39] S Dujko, U Ebert, R D White, and Z L Petrović. Boltzmann equation analysis of electron transport in a N_2-O_2 streamer discharge. *Japanese Journal of Applied Physics*, 50(8S1):08JC01, 2011.

[40] S F Biagi. Monte carlo simulation of electron drift and diffusion in counting gases under the influence of electric and magnetic fields. *Nuclear Instruments and Methods in Physics Research Section A: Accelerators, Spectrometers, Detectors and Associated Equipment*, 421(1):234–240, 1999. Version: 11.2, settings: $1.6 \cdot 10^8$ real collisions, Penning effect not included, Biagi's embedded cross sections.

[41] W Roznerski and K Leja. Electron drift velocity in hydrogen, nitrogen, oxygen, carbon monoxide, carbon dioxide and air at moderate E/N. *Journal of Physics D: Applied Physics*, 17(2):279, 1984.

[42] B H Jeon and Y Nakamura. Measurement of drift velocity and longitudinal diffusion coefficient of electrons in pure oxygen and in oxygen-argon mixtures. *Journal of Physics D: Applied Physics*, 31(17):2145, 1998.

[43] S A J Al-Amin, H N Kucukarpaci, and J Lucas. Electron swarm parameters in oxygen and methane. *Journal of Physics D: Applied Physics*, 18(9):1781, 1985.

[44] JL Hernández-Ávila, E Basurto, and J de Urquijo. Electron transport and ionization in CHF_3–Ar and CHF_3–N_2 gas mixtures. *Journal of Physics D: Applied Physics*, 37(22):3088, 2004.

[45] Pitchford et al. Lxcat: an open-access, web-based platform for data needed for modeling low temperature plasmas. *Plasma Processes and Polymers*, 2016.

[46] H Böhringer, D W Fahey, W Lindinger, F Howorka, F C Fehsenfeld, and D L Albritton. Mobilities of several mass-identified positive and negative ions in air. *International journal of mass spectrometry and ion processes*, 81:45–65, 1987.

[47] R Grünberg. Messungen des Anlagerungskoeffizienten von Elektronen in Sauerstoff. *Zeitschrift für Naturforschung A*, 24(7):1039–1048, 1969.

[48] K Masek, L Laska, and T Ruzicka. Dissociative attachment coefficient in oxygen. *Journal of Physics D Applied Physics*, 10:L25–L28, 1977.

[49] G J M Hagelaar and L C Pitchford. Solving the boltzmann equation to obtain electron transport coefficients and rate coefficients for fluid models. *Plasma Sources Science and Technology*, 14(4):722, 2005. Version: 08/2012, Biagi cross sections from lxcat.

[50] N L Aleksandrov. Three-body electron attachment to a molecule. *Soviet Physics Uspekhi*, 31(2):101, 1988.

[51] B M Smirnov and Harrie S W Massey. *Negative ions*. McGraw-Hill Companies, 1982.

[52] J L Pack and A V Phelps. Electron attachment and detachment. i. pure O_2 at low energy. *The Journal of Chemical Physics*, 44(5):1870–1883, 1966.

[53] L M Chanin, A V Phelps, and M A Biondi. Measurements of the attachment of low-energy electrons to oxygen molecules. *Physical Review*, 128(1):219, 1962.

[54] D W Goodson, R J Corbin, and L Frommhold. Electron avalanches in oxygen: Detachment from the diatomic ion O_2^-. *Physical Review A*, 9(5):2049, 1974.

[55] I Okada, Y Sakai, H Tagashira, and S Sakamoto. Monte carlo simulation of the reaction and transport of negative ions O^- and O_2^- in oxygen. *Journal of Physics D: Applied Physics*, 11(7):1107, 1978.

[56] S W Rayment and J L Moruzzi. Electron detachment studies between O^- ions and nitrogen. *International Journal of Mass Spectrometry and Ion Physics*, 26(3):321–326, 1977.

[57] N L Aleksandrov, S V Kindysheva, I N Kosarev, and A Y Starikovskii. Plasma decay in air and N_2: O_2: CO_2 mixtures at elevated gas temperatures. *Journal of Physics D: Applied Physics*, 41(21):215207, 2008.

[58] N L Aleksandrov and E M Anokhin. Electron detachment from O_2^- ions in oxygen: the effect of vibrational excitation and the effect of electric field. *Journal of Physics B: Atomic, Molecular and Optical Physics*, 44(11):115202, 2011.

[59] A A Ponomarev and N L Aleksandrov. Monte Carlo simulation of electron detachment properties for ions in oxygen and oxygen: nitrogen mixtures. *Plasma Sources Science and Technology*, 24(3):035001, 2015.

[60] L Harrison and J L Moruzzi. Ion mobilities and ion-molecule reaction rates in oxygen. *Journal of Physics D: Applied Physics*, 5(7):1239, 1972.

[61] W Chaibi, R J Peláez, C Blondel, C Drag, and C Delsart. Effect of a magnetic field in photodetachment microscopy. *The European Physical Journal D*, 58(1):29–37, 2010.

[62] J Schiedt and R Weinkauf. Spin-orbit coupling in the O_2^- anion. *Zeitschrift für Naturforschung A*, 50(11):1041–1044, 1995.